



Kinetics of bainitic transformation and transformation plasticity in a high strength quenched and tempered structural steel

R.K. Dutta^{a,*}, M. Amirthalingam^a, M.J.M. Hermans^b, I.M. Richardson^b

^a Materials innovation institute M2i, Mekelweg 2, NL-2628CD Delft, The Netherlands

^b Delft University of Technology, Faculty of 3mE, Mekelweg 2, NL-2628CD Delft, The Netherlands

ARTICLE INFO

Article history:

Received 1 March 2012

Received in revised form

28 May 2012

Accepted 10 August 2012

Available online 6 September 2012

Keywords:

Phase transformation kinetics

Thermomechanical loading

Steel

Bainite

Transformation plasticity

Mechanical characterisation

ABSTRACT

Dilatometric analyses were made on a high strength (830 MPa yield stress) quenched and tempered S690QL1 (Fe–0.16C–0.2Si–0.87Mn–0.33Cr–0.21Mo (wt%)) structural steel during continuous cooling under different mechanical loading conditions. Bainitic transformation kinetics were calculated from the dilatation curves. In addition, the effects of the applied stress on the interface migration velocity, the transformation plasticity and the mechanical driving force for the bainitic transformation were calculated.

The results show that small tensile stresses applied at the transformation temperature do not change the kinetics of the phase transformation or the interface migration velocity. The observed scatter in the interface migration velocity decreases with increasing applied stress due to the transformation induced inhomogeneous plastic deformation. The transformation plasticity increases with increase in the applied tensile stress and the coefficient of transformation plasticity is independent of load. The start temperature for the bainitic transformation decreases upon increasing the applied tensile stress. For a lower starting temperature, more nuclei form during cooling, resulting in a smaller grain size of the bainite phase with increasing tensile stress.

© 2012 Elsevier B.V. All rights reserved.

1. Introduction

S690QL1 is a high strength quenched and tempered structural steel, with a minimum yield strength of 690 MPa and a notch toughness of at least 30 J at $-60\text{ }^{\circ}\text{C}$ [1]. These steels are widely used in welded constructions, such as machines for structural engineering, cranes and bridges. The microstructure of this steel typically consists of tempered martensite in a ferritic matrix, but upon welding, solid state phase transformations occur, accompanied by changes in specific volume. Details of the phase transformation kinetics can be derived from measured dilatation curves [2–4].

During welding or while applying heat-treatments to steel, the transformations generate thermal and metallurgical stresses in the material [5]. Moreover, if the transformation is assisted by an externally applied stress, lower than the yield stress of the weaker phase [5], transformation plasticity occurs. For commercial exploitation and modelling purposes, it is necessary to thoroughly understand the phase transformation behaviour. For precise modelling of the residual stress distribution during welding of such steels, it is essential to fully characterise the phase distribution and associated thermal–mechanical properties. Mohapatra et al. [6] previously studied the transformation plasticity phenomenon during ferritic transformations under tensile loading in the Fe–Ni

system. Further studies were reported for ferrite–austenite transformation in the Fe–Ni system under compressive loading [7,8].

A typical transformation plasticity test [5,9] comprises two consecutive thermal–mechanical cycles on the same specimen; the first is called the free dilatometric cycle, during which the sample has no applied load, the second, undertaken at a constant applied axial force, is referred to as the transformation plasticity cycle. In both cycles, the sample is free to move. However, it may be argued that the first thermal cycle modifies the parent microstructure and the subsequent transformation plasticity cycle is therefore carried out on an altered material. A modified transformation plasticity test is therefore examined within this work. From the dilatation analysis, the effects of the different loading conditions on the kinetics of bainitic transformation in the steel have been analysed and volume fractions of different phases quantitatively evaluated. The interface migration velocity and driving force for the austenite to bainite ($\gamma \rightarrow \alpha_b$) transformation have been calculated and the contribution of the mechanical driving force on the bainite transformation start temperature has been evaluated.

2. Experimental

Table 1 shows the chemical composition of the high strength quenched and tempered S690QL1 steel used in this study. The steel has a grain size of around 40 μm and the microstructure is shown in Fig. 1.

* Corresponding author. Tel.: +31 15 278 22 44; fax: +31 15 278 67 30.
E-mail addresses: r.dutta@m2i.nl, r.k.dutta@tudelft.nl (R.K. Dutta).

Nomenclature

$2\bar{r}_{\alpha_b}$	true average of all grain diameters of bainite, m
$\Delta G^{\gamma \rightarrow \alpha_b}$	free energy change associated with the transformation of austenite to bainite, J mol ⁻¹
ΔG_{Chem}	chemical driving force, J mol ⁻¹
ΔG_{max}	maximum free energy change accompanying the nucleation of bainite, J mol ⁻¹
ΔG_{Mech}	mechanical driving force, J mol ⁻¹
δ	normal component of the transformation strain
$\dot{\epsilon}$	total strain rate, s ⁻¹
$\dot{\epsilon}^e$	elastic strain rate, s ⁻¹
$\dot{\epsilon}^{th}$	thermal strain rate, s ⁻¹
$\dot{\epsilon}^{tp}$	transformation plasticity strain rate, s ⁻¹
$\dot{\epsilon}^{vp}$	viscoplastic strain rate, s ⁻¹
$\Delta V/V$	relative difference of volume between parent and product phases
df_{γ}/dt	kinetics of austenite decomposition, s ⁻¹
ϕ	angle between the stress axis and the normal to the habit plane, deg

σ	magnitude of the applied uniaxial tensile stress, Pa
σ_y^w	yield stress of the weaker phase, Pa
σ_N	resolved normal stress on the habit plane, Pa
σ_y	yield stress, Pa
τ	shear stress resolved on the habit plane in the direction of the shear, Pa
\underline{S}	deviatoric part of the applied stress tensor
ϵ^{tp}	transformation plasticity strain
B_s	bainite start temperature, °C
E	Young's modulus, Pa
f_{α_b}	transformed bainite fraction
G_N	universal nucleation function, J mol ⁻¹
G_{SB}	stored energy of bainite, J mol ⁻¹
k	transformation plasticity coefficient, Pa ⁻¹
s	transformation shear strain
v_{α_b}	interface migration velocity, m s ⁻¹
Z	volume fraction of product phase

2.1. Evaluation of tensile property

Samples for tensile testing at room temperature (Fig. 2a) and elevated temperatures (Fig. 2b) were prepared from the 16 mm thick as-received S690QL1 plates according to the ASTM-E8/E8M-09 [10] standard. Tensile testing at room temperature was carried out in an electro-mechanical Zwick Z100 tensile testing machine with a load cell of 100 kN. Using an extensometer with a gauge length of 20 mm, elongations were recorded for the applied load using data acquisition software TestXpert[®] II. Testing was carried out on three samples, and the results were averaged to improve the measurement statistics.

Tensile testing at elevated temperatures was carried out in a 25 kN MTS servo-hydraulic tensile machine capable of imposing independent temperature and strain profiles on a test specimen. The experimental arrangement for elevated temperature tensile testing is shown in Fig. 3. A high-frequency induction generator was used for heating. Cooling was accomplished by blowing compressed air from three sides onto the specimen and by thermal conduction into the water-cooled specimen grips. The temperature was measured and controlled by three K-type thermocouples that were pressed onto the surface of the specimen at the middle of the gauge length. The contact pressure of the thermocouples was regulated by means of a spring configuration. This leads to a good contact with the specimen surface and an accurate temperature measurement (relative error: ± 1 °C). The maximum temperature variation along the gauge length of the test specimen was less than 10 °C. The axial strain was measured via an air-cooled, high temperature, ceramic rod extensometer with 12 mm gauge length. The MTS thermal-mechanical tensile machine employs a TestStar controller with MultiPurpose Testware[®] (MPT) software to synchronise the multiple control modes required in temperature dependent tensile testing.

Testing was carried at six temperatures, namely 300 °C, 400 °C, 500 °C, 600 °C, 800 °C and 1000 °C until the engineering strain reached 6%. Each test was repeated three times and the results

were averaged to improve the measurement statistics. For temperatures above 500 °C, tests were performed at two different strain rates: 2.5×10^{-3} s⁻¹ and 2.5×10^{-4} s⁻¹. The strain rates were kept constant during the entire tensile test.

2.2. Dilatation properties and extraction of phase transformation kinetics

A Bähr thermoanalysis DIL805 dilatometer was employed for temperature dependent thermal expansion measurements. Samples were milled to $4 \times 10 \times 2$ mm³ to remove the deformation from shear cutting. S-type thermocouples were spot-welded on the samples, both for controlling the heating and the cooling of the sample, and to obtain the temperature profile during the test. The thermal-mechanical cycles employed (Fig. 4b) were used to

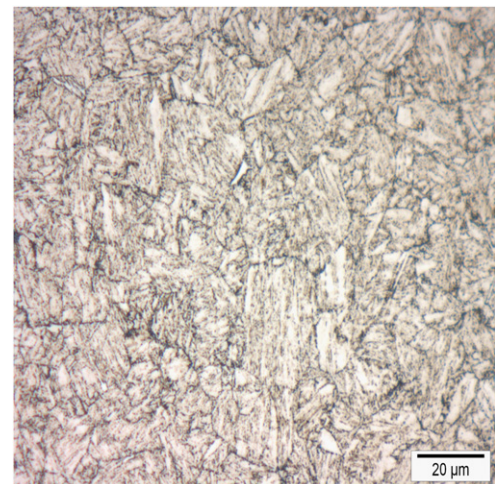


Fig. 1. Microstructure of S690QL1 base metal showing tempered martensite in a ferritic matrix.

Table 1

Chemical composition in wt% of S690QL1 steel.

C	Si	Mn	Ni	P	S	Cr	Mo	N	Nb	Ti	Cu	B	Fe
0.16	0.2	0.87	0.11	0.012	0.001	0.33	0.21	0.0035	0.027	0.005	0.02	0.0021	Bal.

Download English Version:

<https://daneshyari.com/en/article/1576635>

Download Persian Version:

<https://daneshyari.com/article/1576635>

[Daneshyari.com](https://daneshyari.com)